

## Article

# Combustion Characteristics of Small Laminar Flames in an Upward Decreasing Magnetic Field

Yu Xie <sup>1,2</sup>, Zhilong Wei <sup>1</sup>, Teng Zhou <sup>1</sup> , Haishen Zhen <sup>1,\*</sup> , Zihao Liu <sup>1,\*</sup> and Zuohuang Huang <sup>3</sup>

<sup>1</sup> The Mechanical and Electrical Engineering College, Hainan University, Haikou 570228, China; mnyx@leeds.ac.uk (Y.X.); zhilongwei.xjtu@gmail.com (Z.W.); zhouteng@hainanu.edu.cn (T.Z.)

<sup>2</sup> School of Mechanical Engineering, University of Leeds, Leeds LS2 9JT, UK

<sup>3</sup> State Key Laboratory of Multiphase Flows in Power Engineering, Xi'an Jiaotong University, Xi'an 710049, China; zhhuang@mail.xjtu.edu.cn

\* Correspondence: ban18@126.com (H.Z.); fageiliuzihao@126.com (Z.L.)

**Abstract:** The combustion characteristics of laminar biogas premixed and diffusion flames in the presence of upward decreasing magnetic fields have been investigated in this study. The mechanism of magnet–flame interaction in the literature, in which magnetic fields change the behaviors of laminar flames due to the paramagnetic and diamagnetic properties of the constituent gases, is examined and the results are as follows. The magnetic field has no noticeable effect on premixed flames due to low oxygen concentration of the mixed gas at the injection and the relatively high flow momentum. However, due to the diffusion nature of diffusion flames and paramagnetic property of oxygen in ambient air, oxygen distributions are subjected to the gradient of magnetic flux, thus shortening the height of diffusion flames. Results also show that the flame volume is more strongly varied than flame height. Altered oxygen distributions result in improved combustion and higher flame temperature. In the case of current magnet–flame interaction, the magnetic driving force is combined with gravitational force, and a modified gravity  $g^*$  as well as gravity modification factor  $G$  are derived to characterize the paramagnetism theory of oxygen.

**Keywords:** laminar flame; diffusion flame; magnet–flame interaction; paramagnetic oxygen



**Citation:** Xie, Y.; Wei, Z.; Zhou, T.; Zhen, H.; Liu, Z.; Huang, Z.

Combustion Characteristics of Small Laminar Flames in an Upward Decreasing Magnetic Field. *Energies* **2021**, *14*, 1969. <https://doi.org/10.3390/en14071969>

Academic Editor: Roberto Cipollone

Received: 9 March 2021

Accepted: 30 March 2021

Published: 2 April 2021

**Publisher's Note:** MDPI stays neutral with regard to jurisdictional claims in published maps and institutional affiliations.



**Copyright:** © 2021 by the authors. Licensee MDPI, Basel, Switzerland. This article is an open access article distributed under the terms and conditions of the Creative Commons Attribution (CC BY) license (<https://creativecommons.org/licenses/by/4.0/>).

## 1. Introduction

The recent increase in the difficulty of oil extraction and the growing debate over global warming have highlighted the importance of combustion to our civilization. Therefore, it is necessary to have a deep understanding of the combustion process and combustion phenomenon to effectively control such process development. Magnetic fields affect flame behavior because of the paramagnetic and diamagnetic nature of the constituent gases [1,2]. Many studies have been conducted, investigating how the flame behavior is influenced by magnetic fields by using different measurement methods [3–10]. These results demonstrate that magnetic fields can significantly change flame structure [5–14], flame temperature [8,10,15–20], free radical distribution [21–24], flame stability [25,26] and CO/NO<sub>x</sub>/soot emissions as well [6,10,14].

However, understanding the mechanism for magnet–flame interaction is not accomplished overnight. Aoki [5] studied the diffusion flame of butane in a magnetic field generated by an electromagnet. He reckoned that the Lorentz force produced by the presence of charged particles within the magnetic field is not strong enough to cause any significant flame shape deformation. Thus, the Lorentz force is considered to play a negligible role in magnet–flame interaction. Aoki [7] tested butane diffusion flames placed in a uniform-intensity magnetic field, finding that the flame shapes are less affected than the case of magnetic fields with variant intensity. Agarwal et al. [15] also observed that the flame temperature variation is susceptible to gradient magnetic field, whilst a

uniform-intensity magnetic field has negligible influence on flame temperature. The authors suggested that the mechanism of magnet–flame interaction is due to the movement of reactants due to the presence of magnetic field, as a result of which the combustion behaviors of diffusion flames can be changed [27].

Regarding the interaction between flame and a non-uniform magnetic field, more studies have been conducted. Ueno and Harada [12] found that magnetic fields do not concentrate oxygen near the magnet poles but rather seem to arrange oxygen molecules into a “curtain” and thus obstruct the flows of other gases. In the study of a quenching flame by magnetic field, Ueno [28] observed that oxygen is trapped in the region of the highest gradient of magnetic flux. Gilard et al. [26] reasoned that the magnetic force is exerted on oxygen in the air, as its mass magnetic susceptibility is the highest among the species of O<sub>2</sub>, N<sub>2</sub>, H<sub>2</sub>O, CO, and CO<sub>2</sub>. Based on the same reasoning, Gillon et al. [29] proposed that an upward increasing intensity exerts an upward magnetic force on paramagnetic oxygen, whereas a downward increasing intensity would push oxygen down. In both cases, the oxygen concentration in the air around the flame is changed, and the gravitational convective motion of heated air by hot combustion is also altered. In the former case, the flame length was observed to increase [23]. Baker and Calvert [30] examined a laminar diffusion flame in an upward decreasing-intensity magnetic field and observed a significant change in flame behavior where the product of the magnetic field intensity and gradient is sufficiently high.

In the course of understanding the mechanism for magnet–flame interaction, the changes in flame combustion characteristics have been investigated. Wakayama [3] studied the influence of gradient magnetic fields on diffusion flames. Against upward decreasing intensity, the combustion rate of diffusion flames increases. Wakayama et al. [25] reported that gradient magnetic field incurs a convection flow within the flame, whose effect is much similar to the buoyancy effect. Khaldi et al. [31] demonstrated that since the buoyancy effect is induced by the replacement of cold air in the combustion region by hot combustion products, the effect of magnetically induced convection can offset the buoyancy effect on flames by the application of an upward increasing intensity magnetic field. The reason is that oxygen transported by the magnetically induced flow toward the combustion region replaces the combustion products. Therefore, the buoyancy effect is weakened and the flame becomes semi-spherical at some critical magnetic field gradient. In another study, Khaldi et al. [31] associated the intervening effect of magnetically induced convection to buoyancy convection with a parameter of  $F(O_2)$ , defined as the product of the strength of magnetically induced convection and the oxygen concentration. Aoki [6] also conducted a similar study and observed that the flame shape can be compressed into a mushroom shape under a gradient magnetic field with upward increasing intensity.

The above literature review has indicated that only a non-uniform magnetic field can interact with flame, and a small laminar diffusion flame is more affected than a premixed or partially premixed flame. Additionally, the mechanism for magnet–flame interaction is due to the magnetic paramagnetism of oxygen in the air, which is diffused into the flame. However, the combustion characteristics of the flame subject to the influence of magnetic field are not fully understood yet. First, as for flame height change or shape change, which parameter is most sensitive to gradient magnetic field? Second, can flame temperature be varied by gradient magnetic field? Third, as buoyancy effect is closely related to gravitational force, can a better parameter be defined to represent the unified effects of magnetic force and gravitational force? For the purpose of solution, this study aims to experimentally investigate laminar flames interacting with a non-uniform, i.e., upward decreasing magnetic field. By testing both premixed and diffusion biogas flames under gradient magnetic fields, further unique insights into the mechanism of magnet–flame interaction will be gained and elucidate the changes in combustion characteristics of the flames. This study is dedicated to explaining the mechanism of non-uniform magnetic field on the change of flame combustion characteristics and then provides a reference for researchers and engineers of magnetron flame.

## 2. Experimental Setup and Method

Figure 1 schematically shows the experimental apparatus adopted in this study. It comprises the supplies of gases, digital mass flow (DMF) controllers (CS200, accuracy:  $\pm 0.35\%$ , Beijing Sevenstar Flow Co., Ltd., Beijing, China), a burner, two neodymium magnets, and their holder as well as motorized stage, programmable motor controller, B-type thermocouple, data acquisition system, and PC. Metered pure gases of  $\text{CH}_4$ ,  $\text{CO}_2$  with or without dry air enter the single-tube burner with an (inner diameter) ID = 10 mm tube to produce laminar biogas premixed or diffusion flames. The ratio of volume flow rate of methane to carbon dioxide is set as 150%. All gas flows are controlled by DMF controllers, and Table 1 summarizes the flow conditions tested. The exit velocities are the mean velocities estimated based on the mixture mass flow rate at the burner exit. In the case of a premixed flame, the viscosity of the fuel/air mixture has been taken into account to give more accurate velocity. Luminous photos of the flames are taken by a high-resolution.

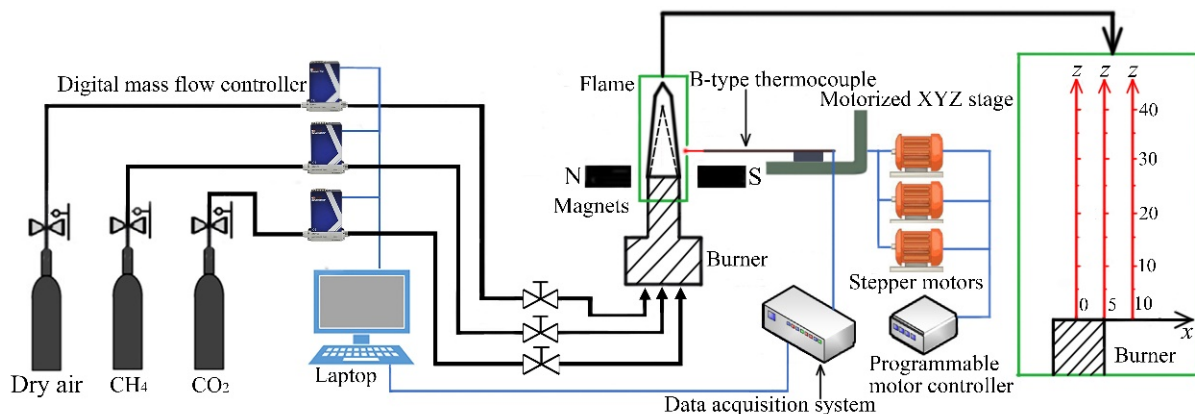


**Figure 1.** Sketch of experimental setup (flames with and without magnetic fields are illustrated by dashed and solid lines, respectively).

**Table 1.** Experimental flow conditions tested.

Types of Small Flames	Reynolds Number	BG <sub>60</sub> Flow Rate (L/min)		Mean Exit Flow Velocity (cm/s)
		CH <sub>4</sub>	CO <sub>2</sub>	
Premixed flame ( $\Phi = 1$ )	428	0.24	0.16	57.0
	321	0.18	0.12	42.7
	214	0.12	0.08	28.5
Diffusion flame	84	0.24	0.16	8.49
	63	0.18	0.12	6.37
	42	0.12	0.08	4.24

Charge-coupled device (CCD) camera with a shutter speed of 1/60 s. The camera head height and burner exit are at the same height in the vertical direction, and the physical length values of the flame are derived from the burner ID (10 mm).

Two identical neodymium magnets having opposite polarities facing each other were used for producing a non-uniform (gradient) magnetic field in this study. Although the coercivity of neodymium magnet decreases rapidly with temperature over 100 °C, and the Curie T is about 320 °C, the distance between magnets and flame heat source is sufficiently far to make sure the magnet temperature is below the critical value. The cross-section of each magnet is 60 mm (length) by 20 (height) mm. The horizontal symmetry line of the magnets was aligned right on the exit plane of the burner port. The center of the cross-section of the magnet is located at the same elevation of the burner exit. The burner

adopted in this study is made of copper (non-magnetic material), which has a negligible effect on the results.

In order to study the effects of non-uniform magnetic fields on premixed or diffusion flames, the distance between two magnets was set at 30 and 20 mm, respectively. Correspondingly, the different magnetic fields achieved were designated as M1 and M2 scenarios. Together with the scenario of no magnets of M0, three scenarios were considered. A digital Teslameter (TD8620, scale: 0–3 T, accuracy  $\pm 1\%$ , Tianheng Measurement and Control Technology Co., Ltd., Changsha, China) was adopted to probe the magnetic field intensity.

A motorized stage (LSCR, made in China, connected to XYZ stepper motors and programmable motor controller) was used to carry the probe of the digital Teslameter. The origin of the axis system is set at the nozzle exit (also the center of magnet system). Thanks to the high precision of positioning and re-positioning of the stage, absolute spatial locations can be visited and revisited. With a pre-programmed code, the magnetic field intensity was measured at 2 mm intervals along three vertical lines located at the radial distances of 0, 5, and 10 mm away from the burner axis, as shown in the fly-out of Figure 1. Once the burner and magnets are fixed in space, the motorized XYZ stage was used to carry the thermocouple for flame temperature measurement. An Omega B-type thermocouple (Chenyi Instrument Co., Ltd., Shenzhen, China, 70%-platinum/30%-rhodium, 0.3 mm bead diameter, 0.225 mm wire diameter) was traversed by the stage to a series of spatial locations, also called grids, where the thermocouple bead was moved. The thermocouple wires are supported by quartz tubes with no shield steel or iron; thus, no influence of the magnetic field on the measurement of temperature is expected. With a pre-programmed code, the stage works in a stop-go-stop mode so that all temperatures of the grids can be automatically registered. At each grid, a total of 50 temperatures were recorded in the stop mode, and the averaged values were reported in this study. All data of temperature are corrected for both conduction and radiation losses.

In this study, each measurement was conducted three times. Using a 95% confidence level, the maximum uncertainties are 3% in magnetic intensity measurement, 8% in flame temperature measurement, and 2% in flame height measurement.

### 3. Results and Discussions

The results of this study are discussed in four subsections. The first is the data the current magnets generate. The second is concerned with visual feature of the flame inside the gradient magnetic field and the analysis of flame temperature. The third deals with the establishment of a mathematical model for the volume of the flame based on the integrated flame surface as well as its variation relative to the magnetic field gradient. The fourth is about the changed temperature distributions under different scenarios of magnetic field gradients. The last focuses on the competition between the effect of magnetically induced convection and buoyancy convection and the usage of a parameter, i.e., integrated gravity, to characterize such a combined effect.

#### 3.1. Data of Current Magnets

This study is to explore the gravity effect ( $z$ -axis direction) of a non-uniform magnetic field on flame; consequently, the vertical ( $z$ -axis direction) distributions of magnetic field intensity in M1 and M2 scenarios are given in Figure 2, from which the gradient of magnetic flux in the  $z$ -axis direction can be calculated by  $B_z dB_z/dz$  (see Equation (5) and is also presented in Figure 2. As shown by the figure, the magnetic field intensity is the maximum at the burner exit ( $z = 0$  mm). Then, the field intensity decreases steeply upwards. In addition, a comparison of the field intensities of  $x = 0, 5, 10$  mm at the same  $z$  indicates that the intensity increases with the increase of radial distance at low elevations. Especially at  $z = 0$  mm, the magnetic field intensity increases most rapidly with increasing  $x$  from 0 to 10 mm. While at high elevations of  $\approx 20$  mm, the intensities approach 0 T faster at a further radial distance. As for the gradient of magnetic flux, its strength (absolute value) in the scenarios of M1 and M2 arrives at the maximum near the burner exit ( $z = 6$  mm). Then, a

monotonic decay of the gradient of magnetic flux versus increasing elevation is observed. Note that as the flame resides on the vertical symmetry line of the system, no influence is expected to the symmetrical nature of the flame.

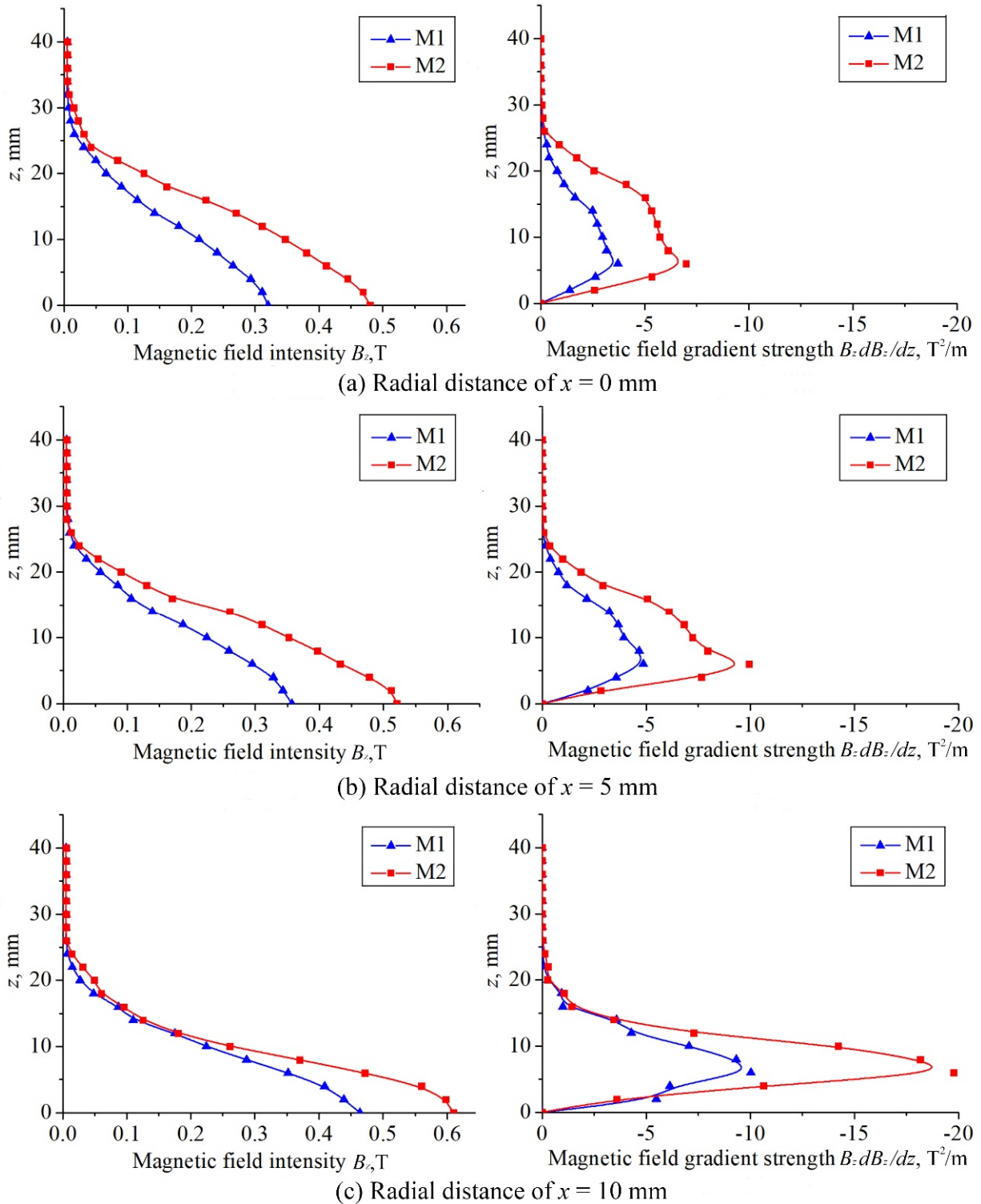


**Figure 2.** Vertical distributions of magnetic field intensity and gradient along three lines in Figure 1 at (a)  $x = 0$  mm, (b)  $x = 5$  mm, and (c)  $x = 10$  mm, respectively.

### 3.2. Effect of Magnetic Field on Flame Shape

Under three scenarios of upward decreasing magnetic fields (M0, M1, and M2), both premixed and diffusion flames are established according to the flow conditions in Table 1. As shown, three jet flow Reynolds numbers or three flames are tested for either premixed or diffusion flame. The highest Reynolds number is 428, and thus, both premixed and diffusion flames are small flames in the laminar regime. Figure 3 shows the visual photos of the flames. The heights in the case of the premixed flame are 16, 12, and 9 mm for constant Reynolds numbers of 84, 63, and 42, respectively. As seen, each diffusion flame is of an inverted U shape. There is a decrease in diffusion flame height against the magnetic field scenarios of M0, M1, and M2, and meanwhile, the flame profile shrinks inwards. In contrast, the premixed flame is of a cone shape, with its height negligibly changed when two magnetic fields (M1 and M2) are applied. The heights in the case of the diffusion flame are 58–52, 42–39, and 29–26 mm for constant Reynolds numbers of 84, 63, and 42, respectively. Figure 2 has revealed that the region with strong magnetic field intensity and gradient of magnetic flux is  $z < 30$  mm. Thus, except for the flame at  $Re = 42$ , the other flames are so long that the heights extend beyond the region of  $z < 30$  mm. Within such a region of strong magnet–flame interaction, the middle waist part of the flame is shrunk inward significantly.

According to the interaction mechanism of a non-uniform magnetic field and paramagnetic oxygen, the additional flow of ambient oxygen forced by the gradient magnetic field accelerates the mixing between the flame jet and ambient air, which would improve the combustion of fuel in the case of a diffusion flame. Due to the downward convection of ambient oxygen induced by the gradient magnetic field, the flame is prone to be compressed, leading to a shorter flame height. The effect of compression due to magnetic force is also clear by the observation of the shrinking waist of the flame profile. This is straightforward that as the gradient of magnetic flux is increased toward the region near the burner exit ( $z = 6$  mm), the paramagnetic force on ambient oxygen is the largest thereunto, and the distortion of flame shape will also be most significant.

In addition, the more obvious difference between M0, M1, and M2 is the thickness of the reaction zone. At different Reynolds numbers, as shown in Figure 3, the bright region of M2 (estimated as reaction region) is thicker than that of M0. Based on the same exposure time of the two images, the brightness of the M2 reaction area is also higher than that of M0. The difference of the reaction zone should be more related to oxygen entrainment and temperature rise.

### 3.3. Effect of Magnetic Field on Volume of the Flame Based on the Integrated Flame Surface

As the findings in Section 3.2 show, the variation in the height and width of a small laminar diffusion flame under a gradient magnetic field is visibly noticeable to the naked eye. It is conventional to report flame height and width, which can be directly measured [5–14]. However, according to the magnet–flame interaction, it is a body force exerted from the magnetic field gradient on the paramagnetic oxygen. As a result of the redistribution of oxygen in space, the envelope of the flame is changed three-dimensionally. Thus, it would be of greater significance to examine the change in volume of the flame based on the integrated flame surface due to the effect of the gradient magnetic field, instead of flame height or width. Figure 3 indicates that except for the reduction of flame height, the shrinkage in flame profile is almost axisymmetric, and such inward shrinkage will further reduce the volume of the flame based on the integrated flame surface. To acquire this, the details of the 2D flame profile curve need to be firstly defined, based on which an integration against flame height ( $x_f$ ) would be applied. The horizontal force that is directed outwards (deducted by the horizontal gradient, as seen in Equation (2)) would be offset on a general scale, so it is reasonable to assume that the flame maintains its axisymmetric nature.

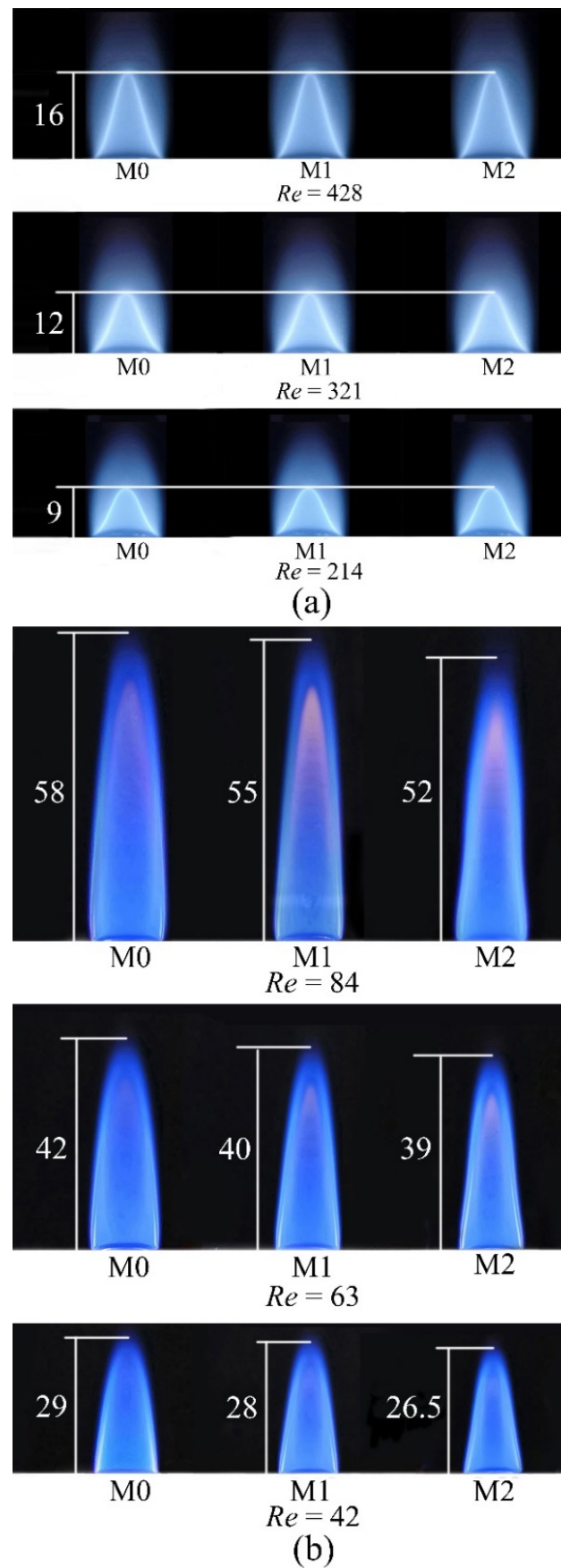


**Figure 3.** Photos of (a) premixed flames and (b) diffusion flames of different Reynolds numbers in three scenarios of magnetic fields (white numbers are flame heights with the unit of mm).

For combustion of a biogas diffusion flame, most parts of the flame are the color blue because of weak sooting. Thus, the length of the outermost blue profile of the flame that is indicative of CH radical emission is defined as the flame length in this study. The raw pictures of the blue flames are binarized and then reversed to get the flame profiles by the MATLAB edge detector program. Consequently, the flame heights can be obtained by MATLAB. The polynomial fitting of flame profiles was made by selecting 15 points evenly distributed along each profile. Next, quadric polynomial fitting (fourth-order polynomial fitting) was applied, which can coincide with the profiles very well, as shown in Figure 4. The obtained equations of the profiles are integrated to arrive at the volume by:

$$V_f = \int_0^{x_f} \pi f(x)^2 dx \quad (1)$$

where  $V_f$  is volume of the flame based on the integrated flame surface,  $x_f$  is flame height, and  $f(x)$  is the fitted curve of each flame profile.

The variations of the flame heights and integrated volumes under different gradients of magnetic fields are given in Figure 5. It is revealed that when the gradient increases from M0 to M1 and further to M2, both flame height and volume exhibit a trend of decrease. Compared with the decrease rate of flame height, the volume of the flame based on the integrated flame surface has a faster rate of decline, which means that the parameter of volume is more sensitive to the magnetic field gradient. Therefore, although the parameter of flame height can be measured directly, the volume of the flame based on the integrated flame surface is an alternative indicator for studying magnet–flame interaction. The reason is that the force induced by the magnetic field to both ambient oxygen and the oxygen diffused into the flame is a volumetric force in nature [31,32]. So, it can be suggested to derive the parameter of volume by integration for analysis of magnet–flame interaction. Potentially, the volume of the flame based on the integrated flame surface derived can be adopted for a deeper understanding of the mechanism of magnet–flame interaction.

### 3.4. Temperature Distribution Variations

#### 3.4.1. Centerline Temperature Distributions at Different Elevations

The temperature distributions along the flame centerline under three scenarios of magnetic fields are presented in Figure 6. With increasing elevation ( $z$ ), the temperature surges first and then increases moderately, after which temperature decay occurs, respectively corresponding to the preheating/initial-combustion, main combustion, and post-combustion zones of the diffusion flame. In each zone and compared to the temperatures without a magnetic field, the temperatures under magnetic fields exhibit an increase in the main combustion and post-combustion zones. Meanwhile, the magnetic field of M2 incurs a larger temperature rise than that of M1. The reason for such temperature increase is a higher mole fraction of oxygen inside the flame as a result of an increased diffusion of ambient oxygen into the flame [30]. According to the magnetic susceptibility of paramagnetic oxygen, oxygen is moved toward the direction of a higher gradient of magnetic flux within the magnetic field. Meanwhile, the combustion products are diamagnetic gases having opposite susceptibility of oxygen and thus are pushed to the opposite direction of the magnetic field. The combined effect is a larger mole fraction of oxygen in the combustion region of the diffusion flame. As the combustion is rich in fuel in the main combustion zone, which is at the middle of the flame and has better fuel/air mixing than its upstream preheating/initial-combustion zone, the main combustion is enhanced by both oxygen addition and the removal of combustion products. Following the temperature increases in the combustion zone, the temperatures in both upstream preheating and post-combustion zones also show a trend of increase.

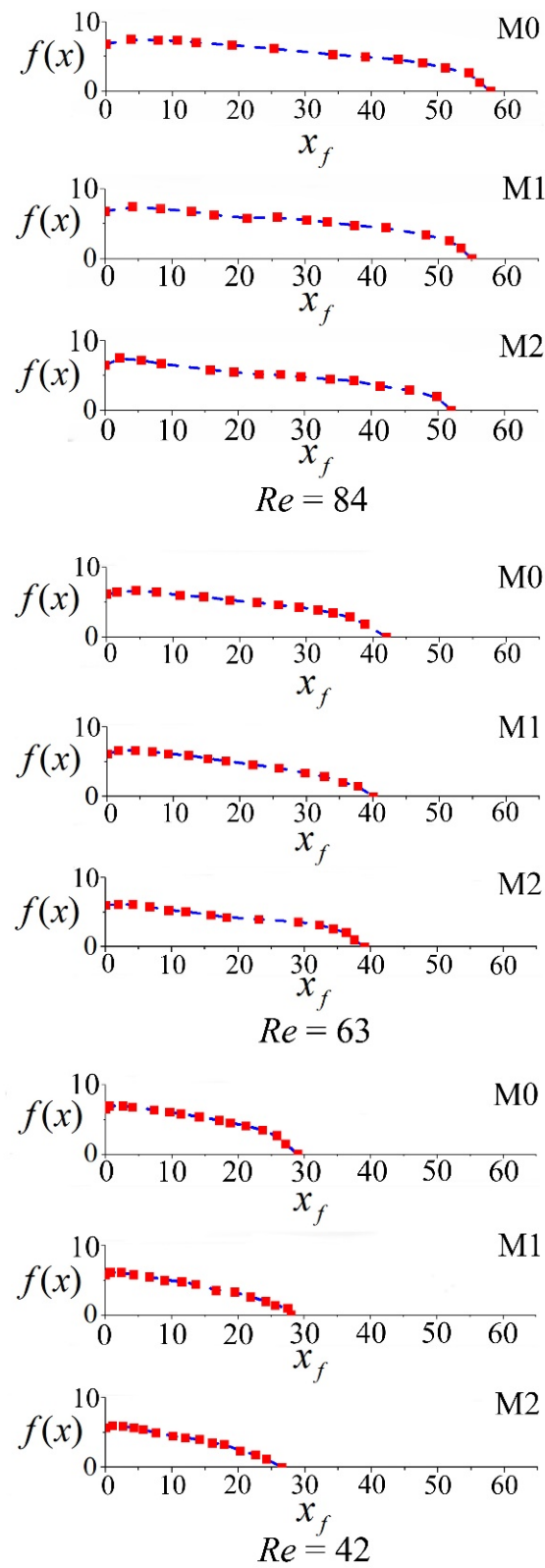


**Figure 4.** Profiles of diffusion flames under different scenarios of magnetic fields (red squares are selected points for curve fitting; blue lines are fitted curves about  $x_f$ ).

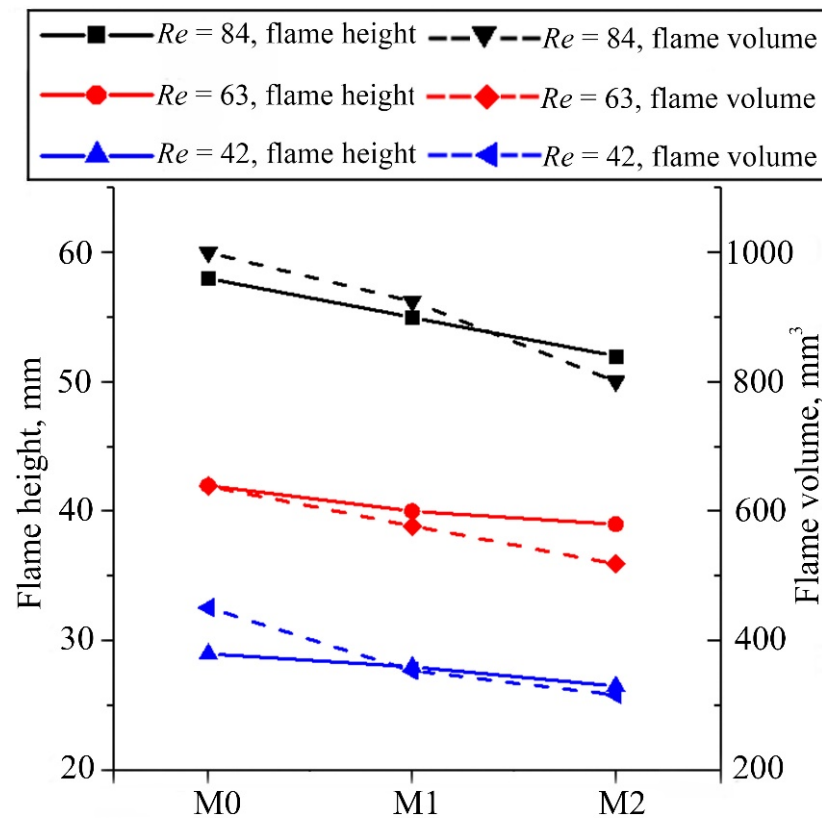


**Figure 5.** Effects of different gradient strengths of magnetic fields on height and volume of diffusion flames.

### 3.4.2. Radial Temperature Distributions

Now, it is seen that the height, width, volume, and centerline temperature of the small laminar diffusion flame can be altered by a gradient magnetic field. Actually, a change in the former three quantities can incur changes to flame temperature distributions. That is, a change in flame height or width alone would change the flame temperature field. As flame temperature is an important indicator of combustion condition, so in order to obtain more information about the change of combustion condition caused by a gradient magnetic field, more quantitative analysis of the temperature distributions is necessary. The motorized XYZ stage can be used to detect the temperature change ascribable to its shape distortion, which has been successfully used in Reference [33]. In this study, the same method was used to further analyze the reasons for temperature distribution change under a gradient magnetic field.

Considering the fact that the vertical scope of the strong magnetic field gradient is within the range of  $z < 30$  mm and that the diffusion flame under  $Re = 42$  is the shortest among all, its radial temperature distribution is expected to be most significantly changed. To obtain the radial temperature distributions, a total of 21 rows of grids at different elevations were adopted with the motorized XYZ stage traversing the thermocouple along each row. Note that located in each row were eight grids, thus engendering a rectangular array of 168 grids in total. The lowest row of this array was horizontally at  $z = 0$  mm, and the others were located with an increment of  $z = 2$  mm.

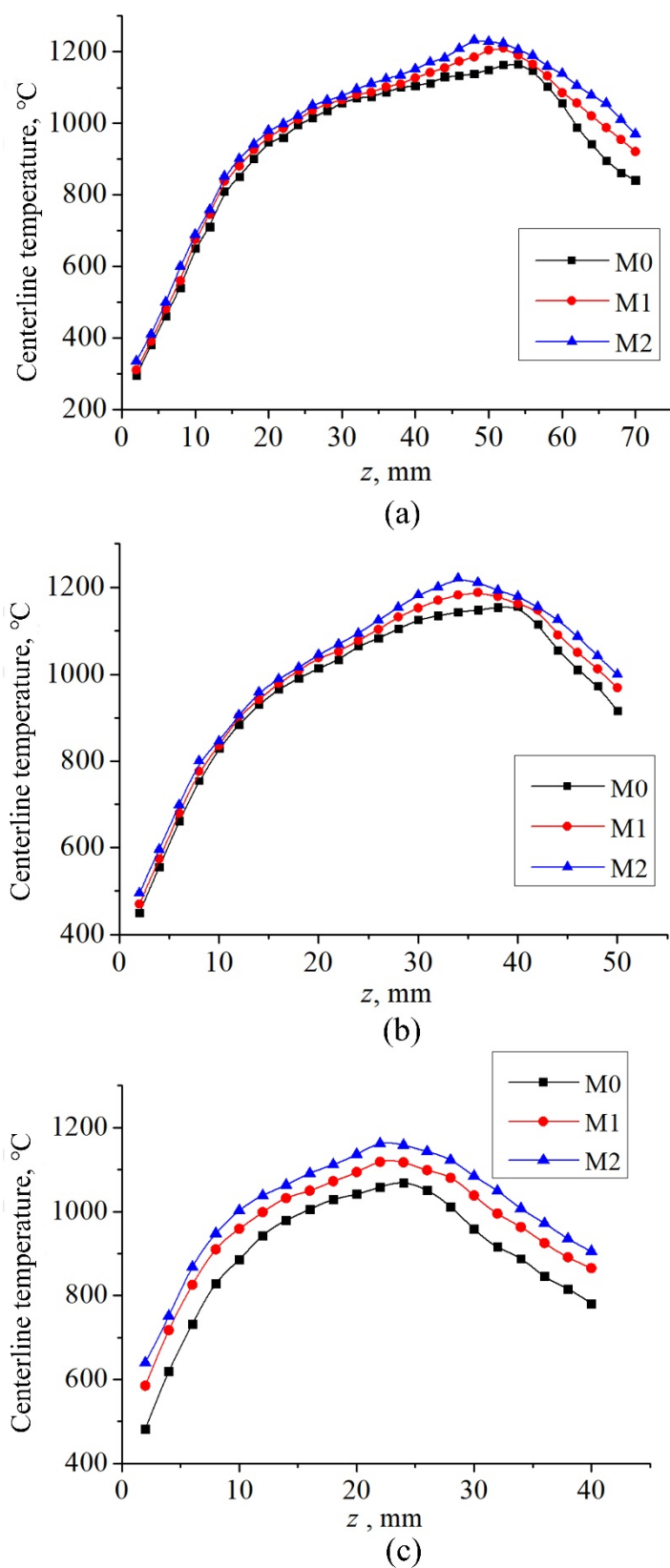


Figure 6. Centerline temperature distributions of diffusion flames: (a)  $Re = 84$ , (b)  $Re = 63$ , and (c)  $Re = 42$ .

In three scenarios of magnetic fields, the radial temperature distributions obtained are shown in Figure 7. As the distortion in flame shape mainly occurs at the upper half of the

flame, the data in the 6th row represent the distribution features from the 1st to 10th row. The data from the 17th to 20th rows are also omitted in Figure 7 due to the same reason. To provide a baseline for discussion, a black dashed line is shown in each figure to denote the radial location of the flame/air interface in the scenario of M0, i.e., the flame under no magnetic field. At  $z = 10$  mm in Figure 7a, the magnetic fields of M2 and M1 incur a similar temperature rise over  $100$  °C at the radial distance from the flame axis of  $0 \text{ mm} \leq x < 3 \text{ mm}$ . Note that the grids at  $0 \leq x \leq 4 \text{ mm}$  are inside the flame in all three scenarios. For the grids outside the flames at  $x \geq 6 \text{ mm}$ , the temperatures show no perceptible change. At  $z = 10 \text{ mm}$  and  $0 \text{ mm} \leq x < 6 \text{ mm}$  in Figure 7b, the magnetic fields of both M1 and M2 show an enhancement effect on flame temperature compared to the magnetic field of M0, and further, the magnetic field of M2 induces a larger temperature increase than M1. Note that the temperature difference occurs both inside the flame at  $x \leq 2 \text{ mm}$  and outside the flame at  $4 \text{ mm} \leq x < 6 \text{ mm}$ , while with no perceptible temperature difference at  $x > 6 \text{ mm}$ . In Figure 7c,d, the temperature distributions both inside and outside the flame in M2 show a much more significant rise than the cases of M1 and M0. Note that the temperatures at the grids of  $4 \text{ mm} \leq x < 10 \text{ mm}$  in Figure 7c or  $4 \text{ mm} \leq x \leq 10 \text{ mm}$  in Figure 7d, which are outside the flame, still increase when M1 and M2 magnetic fields are applied. Similarly, the increases of temperatures outside the flame can be observed at  $2 \text{ mm} \leq x < 10 \text{ mm}$  in Figure 7e,f. The visual photos in Figure 3 have indicated that the flame height shortens and the profile shrinks from M0 to M1 and M2. Therefore, the sole effect of distorted flame shape on radial flame temperature would be that for the grids outside the flame, the temperature recorded by the thermocouple will drop as it is “moved” away from the flame. In other words, the temperatures registered outside the flame are expected to drop as the shortening and shrinking flame gets away from the grid/thermocouple. However, the fact is to the contrary of such expectation. The only reason for the increased temperature outside the flame is that the temperature within the flame is enhanced. As discussed before, the higher temperature inside the flame is a result of improved combustion due to a higher fraction of oxygen promoted by the magnetic field effect. This explanation is consistent with Reference [15] that a non-uniform magnetic field will incur a rearrangement of oxygen concentration in the radial direction, leading to a temperature rise within the flame. This is also in good agreement with Reference [12], reporting that instead of concentrating oxygen near the magnetic poles, a strong field gradient of magnetic flux lines up oxygen to reduce the flow of other gases between the poles. Figure 7 further shows that for the rows of grids above the flame height at  $z = 30$  and  $40 \text{ mm}$ , the difference in radial temperatures becomes smaller toward higher elevation. This is because the temperature outside the flame is subject to rapid mixing between a hot combustion product and ambient cold air, which minimizes the temperature difference. However, the hotter flame in the scenarios with a magnetic field is still obvious, which is indicative of improved combustion by the application of a gradient magnetic field.

### 3.5. Reinforced Gravity Effect of Current Magnetic Field on Flame

Since the magnet–flame interaction is through the means of a magnetic body force exerted on gases, its nature is rather similar to the gravitational force on the gases. Similar to buoyancy flow convection driven by gravity in non-isothermal fluids due to the variation in flow gas density with temperature, the magnet-induced flow convection is driven magnetically due to the spatial variations in paramagnetic susceptibilities of non-isothermal fluids. According to Reference [34], the body force of a gas in the gradient magnetic field of this study,  $F_m$ , is

$$F_m = \frac{1}{2\mu_0} \rho \chi_m \nabla B^2 \quad (2)$$

where  $\rho$  is the density of the gas,  $\mu_0$  is the vacuum permeability ( $\mu_0 = 4 \times \pi \times 10^{-7} \text{ N/A}^2$  [26]),  $\chi_m$  is the magnetic susceptibility of the gas,  $\nabla B^2$  is the gradient of square magnetic flux density, and  $B$  is the magnetic field intensity.

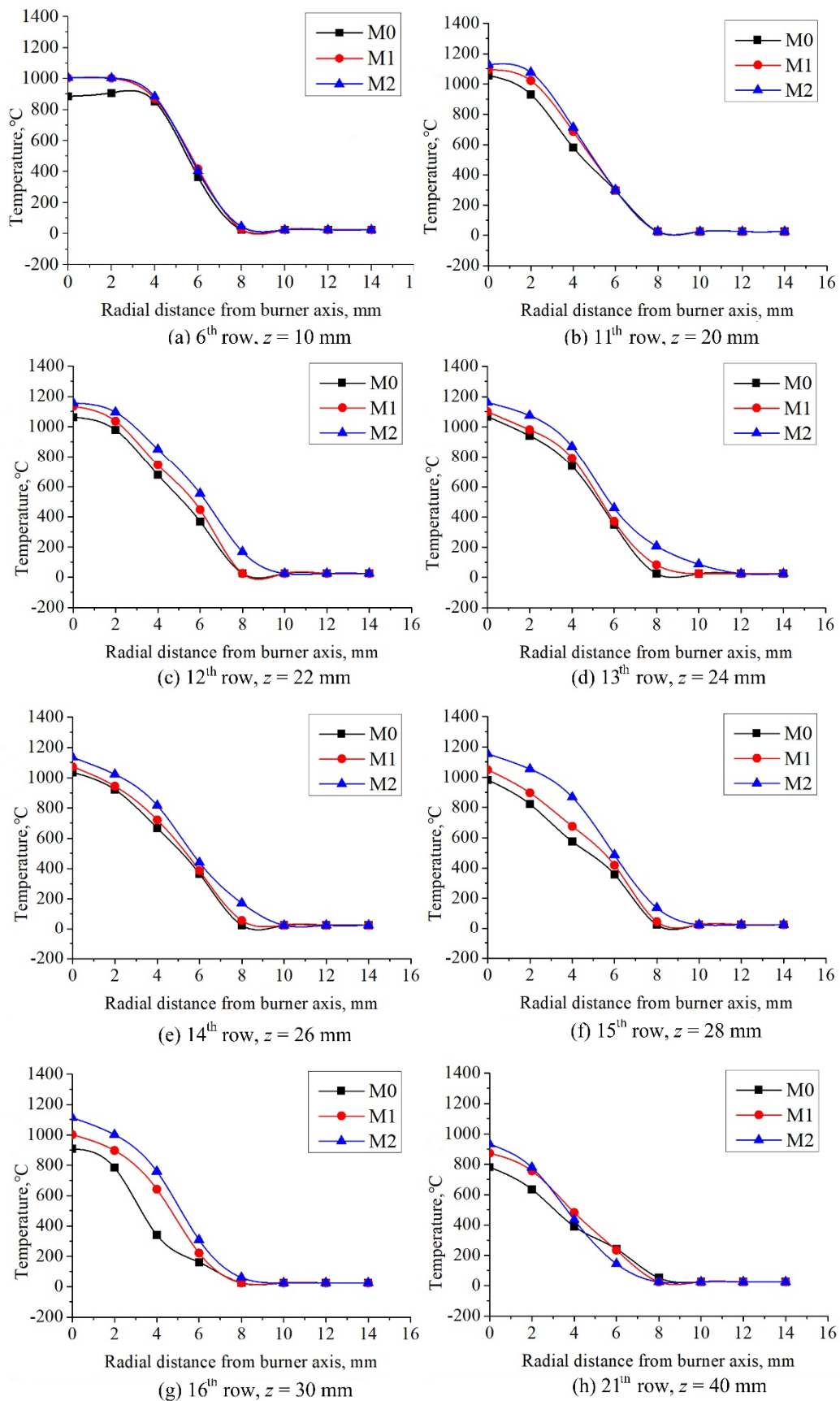
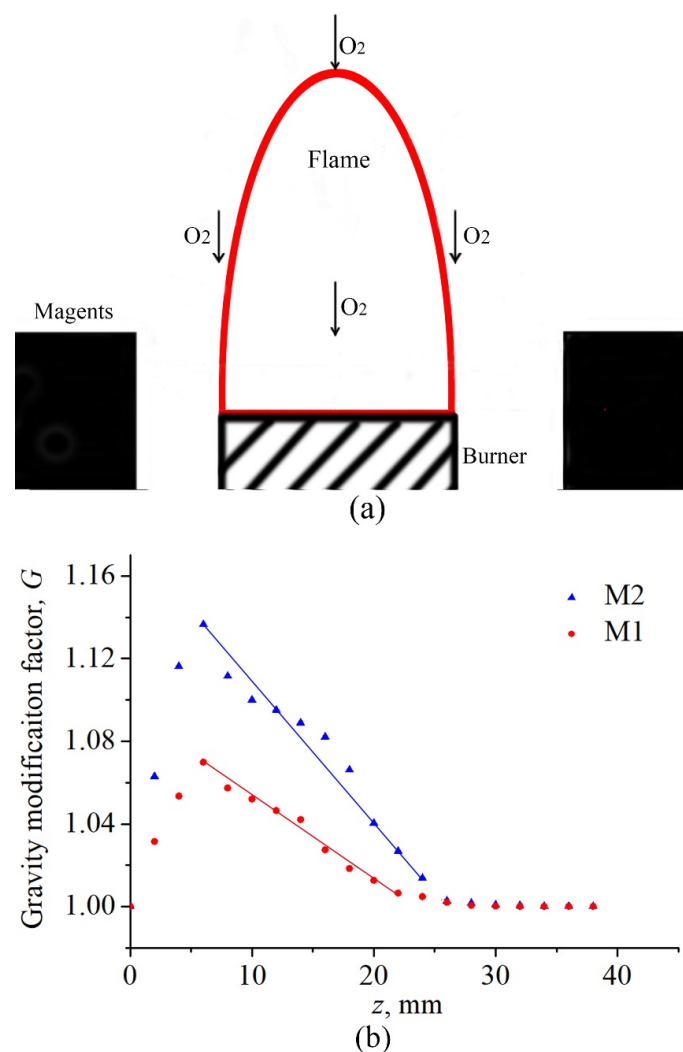


Figure 7. Radial temperature distributions at different elevations of diffusion flame at  $Re = 42$ .

As the magnetic susceptibility of oxygen is the largest among all constituent gases of the flame, the magnetization force on other gases can be ignored. That is, the magnetic body force created by the gradient magnetic field on all gases can be assumed equal to that on oxygen only. In this regard, the force acting on oxygen in ambient air is of a much higher magnitude than the force on oxygen inside the flame, since the oxygen concentration outside the flame is much higher than that inside the flame. Figure 8a qualitatively illustrates the magnetic forces on both the external and internal gases ( $O_2$ ) of the diffusion flame in the  $z$ -axis direction. Therefore, the flame is contracted, the height is decreased, and the integrated volume is depressed, which is mainly due to an overall downward-pushing force from external gases that are driven by the gradient magnetic field. As discussed, oxygen inside the flame is also driven by the magnetic force, giving rise to an overall vertically downward force acting on the whole body of the flame. As reported in the literature [34,35], this force intervenes in the gravitational force, which influences the buoyancy effect. Therefore, it is necessary to further examine how these two forces interact with each other in this study. Starting with Equation (2) and considering the internal oxygen of the flame along the symmetry line, the intervening effect of magnet-induced convection to gravity-induced convection can be proved to be characterized by a parameter of gravity modification factor  $G$ , whose derivation and validation process is as follows.



**Figure 8.** (a) Illustration of magnetic forces on oxygen inside and outside the flame: The vertical direction indicated by the black arrow is the force direction of oxygen; (b) Reinforced gravity effect in terms of gravity modification factor  $G$  versus elevation.

Firstly, to take into account both gravitational force and magnetic force for convection, a modified gravity  $g^*$  can be defined:

$$g^* = g_m + g \quad (3)$$

where  $g$  is the terrestrial gravity ( $g = 9.7863 \text{ m/s}^2$ , in Haikou city, China). The degree of modification of gravity  $g$  can be characterized by a dimensionless number,  $G$ :

$$G = g^*/g \quad (4)$$

Now, we have defined modified gravity of  $g^*$  and gravity modification factor  $G$  to represent the combined effects of magnetically induced convection and gravitationally induced convection. Then, the acceleration of internal oxygen caused by the magnetic force can be calculated, according to Reference [35]:

$$g_m = \frac{\chi_m}{2\mu_0} \frac{\partial B_z^2}{\partial z} = \frac{\chi_m}{\mu_0} B_z dB_z/dz \quad (5)$$

where  $\chi_m$  is:

$$\chi_m = \frac{\chi_v}{\rho} \quad (6)$$

and  $\chi_v$  is the volume magnetic susceptibility of gas [36,37]. According to References [38–40],  $\chi_v$  can be deduced from the following expression:

$$\chi_v = \frac{M}{B} = \frac{CB/T}{B} = C/T \quad (7)$$

where  $M$  is the resulting magnetization,  $T$  is the absolute temperature, and  $C$  is the material-specific Curie constant. According to Reference [15], the value of  $C$  for oxygen is  $393 \times 10^{-6} \text{ K}$ .

It is clear from these equations that the magnetic force on internal oxygen is proportionally related to the gradient of magnetic flux, and it is reversely related to flame temperature. Specifically, the characteristics of laminar diffusion flame can be significantly changed when the gradient of magnetic flux, i.e.,  $B_z dB_z/dz$  is large, and furthermore, when the flame temperature becomes higher, the changes in flame characteristics are lessened due to a reduction in the mass susceptibility of oxygen.

To study the validity and physical meaning of  $G$ , the diffusion flame under  $Re = 42$ , which is totally within the scope of significant magnetic field effect at  $z < 30 \text{ mm}$ , is adopted. First, at different elevations of the flame, the values of gradient of magnetic flux are coupled with flame temperatures to yield the values of  $g_m$ . Then, using Equations (3) and (4), the value of  $G$  can be obtained. Figure 8b gives the variations of  $G$  versus elevation at constant  $x = 0 \text{ mm}$ . As seen in either scenario of M1 and M2, the data points of  $G$  at  $z > 4 \text{ mm}$  can be well fitted by a linear line, and the value of  $G$  monotonically decreases toward 1 and becomes 1 at  $z > 26 \text{ mm}$ . Note that  $g^* = g$  and  $G = 1$  in the absence of a magnetic field. The linear decay of  $G$  reveals that the force of the magnetic field on internal oxygen gradually decays with increasing elevation. The overall magnetic force exerted on the whole body of the flame develops downwards, reinforcing gravity, and thus strengthening the buoyancy effect. In this regard, the linear decay of  $G$  means that the modification in gravity or buoyancy effect is lessened at a higher elevation. Furthermore, the slope of the line characterizes the rate of such modification. The larger the magnetic field gradient, the steeper the line, and the larger the slope. The best fitting expressions ( $4 \text{ mm} < z < 24 \text{ mm}$ ) for two scenarios are:

$$G = -0.0041z + 1.095, R^2 = 0.98 \text{ --- M1} \quad (8)$$

$$G = -0.0067z + 1.167, R^2 = 0.95 \text{ --- M2} \quad (9)$$

Therefore, the fittings in Figure 8b are very justified with  $R^2$  both over 0.95, which are appropriate for predicting the relationships between  $G$  and  $z$ .

Now, based on the present experimental data of the magnetic flux gradient and flame temperature, modified gravity  $g^*$  as well as gravity modification factor  $G$  have been introduced. Their physical meanings agree well with the paramagnetism theory of oxygen and the mechanism of magnet–flame interaction in the literature. Hence, they are effective parameters to quantify the interaction between small laminar diffusion flame and non-uniform magnetic field, especially within the scope of experimental configurations and conditions tested in this study.

#### 4. Conclusions

In this work, the interactions between upward decreasing magnetic fields with small, laminar flames were experimentally investigated. Both premixed and diffusion flames were tested. The main findings are as follows:

- (1) The mechanism of magnet–flame interaction reported in the literature supports that a non-uniform magnetic field interacts with a flame due to the susceptibility of oxygen to a gradient magnetic field. In the current upward decreasing magnetic field, the paramagnetic force on oxygen makes oxygen distributions around the flame altered. In the case of premixed combustion (equivalence ratio equals 1), no obvious changes occur in flame behavior due to low oxygen concentration of the mixed gas at the injection and the relatively high flow momentum. While for diffusion combustion, flame behaviors are significantly changed.
- (2) By using the MATLAB edge detector program to identify the profile of the diffusion flame and polynomially fitting the profile, the volume of the flame based on the integrated flame surface is obtained. Both the height of the diffusion flame and volume of the flame based on the integrated flame surface show a decrease as the gradient of magnetic flux increases. Examination of the effect of the magnetic field on the flame shows that the volume of the flame based on the integrated flame surface is more sensitive to the gradient magnetic field than the flame height.
- (3) The temperatures along the flame centerline show a trend of increase with the increasing gradient of magnetic flux from the scenario of M0 to M1 and further to M2. Moreover, the scenario of M2 incurs a larger temperature enhancement than M1. The reason for the temperature increase is that oxygen is attracted toward the direction of higher magnetic field gradient, promoting the diffusion of ambient oxygen into the combustion zone, resulting in more complete combustion. With the aid of motorized XYZ stage, the temperatures at 2D spatial grids inside and outside the flame are monitored. The results confirm that temperature increases are a result of a higher molar fraction of oxygen, which caused diffused oxygen into the flame.
- (4) A modified gravity  $g^*$  is used as a combination of  $g$  and  $g_m$ , where  $g_m$  describes the vertical magnet-induced mass acceleration of oxygen due to the paramagnetic force acting on oxygen. A dimensionless number  $G$  quantifies the competing buoyancy-induced and magnet-induced convection. The parameters proposed both qualitatively and quantitatively coincide with the experimental data of this study.

**Author Contributions:** Conceptualization, Y.X. and H.Z.; Methodology, Y.X. and Z.L.; Validation, Z.L.; Formal analysis, Y.X.; Investigation, Y.X. and T.Z.; resources, Z.L. and H.Z.; Data curation, H.Z., Z.W. and T.Z.; Writing—original draft preparation, Y.X.; Writing—review and editing, H.Z.; Visualization, Y.X.; Supervision, H.Z.; Project administration Z.H.; Funding acquisition, Z.L. All authors have read and agreed to the published version of the manuscript.

**Funding:** This research was funded by the Hainan Provincial Natural Science Foundation of China (519MS023) and National Natural Science Foundation of China (51766003).

**Institutional Review Board Statement:** Not Applicable.

**Informed Consent Statement:** Not Applicable.

**Data Availability Statement:** Data sharing is not applicable to this article.

**Acknowledgments:** The authors thank Hainan Provincial Natural Science Foundation of China (519MS023) and National Natural Science Foundation of China (51766003) for financial support of the present study.

**Conflicts of Interest:** The authors declare no conflict of interest.

## Nomenclature

B	magnetic field intensity, T
$\nabla B^2$	gradient of square magnetic flux density, T <sup>2</sup> /m.
C	material-specific Curie constant, K
d	inner diameter of the nozzle, mm
g	terrestrial gravity, m/s <sup>2</sup>
g*	modified gravity, m/s <sup>2</sup>
g <sub>m</sub>	vertical magnetic mass acceleration of gas, m <sup>2</sup> /s
ID	inner diameter of burner, mm
F <sub>m</sub>	magnetic body force of gas, N/m <sup>3</sup>
G	dimensionless number of g* relative to g
M	resulting magnetization, A/m
T	absolute temperature, K
V <sub>f</sub>	volume of the flame based on the integrated flame surface, mm <sup>3</sup>
x	radial distance from burner axis, mm
x <sub>f</sub>	flame height, mm
z	height above burner port, mm
Greek Symbols	
ρ	mass density of gas, kg/m <sup>3</sup>
χ <sub>m</sub>	mass magnetic susceptibility of gas, m <sup>3</sup> /kg
χ <sub>v</sub>	volume magnetic susceptibility of gas
μ <sub>0</sub>	vacuum permeability, N/A <sup>2</sup>

## References

- Ueno, S.; Esaki, H.; Harada, K. Magnetic Field Effects on Combustion. *IEEE Transl. J. Magn. Jpn.* **1987**, *2*, 861–862. [[CrossRef](#)]
- Wakayama, N.I. Behavior of gas flow under gradient magnetic fields. *J. Appl. Phys.* **1991**, *69*, 2734–2736. [[CrossRef](#)]
- Wakayama, N.I. Magnetic promotion of combustion in diffusion flames. *Combust. Flame* **1993**, *93*, 207–214. [[CrossRef](#)]
- Wakayama, N. Magnetic acceleration and deceleration of O<sub>2</sub>/gas streams injected into air. *IEEE Trans. Magn.* **1995**, *31*, 897–901. [[CrossRef](#)]
- Aoki, T. Radicals' Emissions and Butane Diffusion Flames Exposed to Upward-Decreasing Magnetic Fields. *Jpn. J. Appl. Phys.* **1989**, *28*, 776–785. [[CrossRef](#)]
- Aoki, T. Radical Emissions and Anomalous Reverse Flames Appearing in Upward-Increasing Magnetic Fields. *Jpn. J. Appl. Phys.* **1990**, *29*, 181–190. [[CrossRef](#)]
- Aoki, T. Radical Emissions and Butane Diffusion Flames Exposed to Uniform Magnetic Fields Encircled by Magnetic Gradient Fields. *Jpn. J. Appl. Phys.* **1990**, *29*, 952–957. [[CrossRef](#)]
- Sharma, S.; Sheoran, G.; Shakher, C. Temperature measurement of axisymmetric flame under the influence of magnetic field using lensless Fourier transform digital holography. *Appl. Opt.* **2012**, *51*, 4554–4562. [[CrossRef](#)]
- Kumar, M.; Agarwal, S.; Kumar, V.; Khan, G.S.; Shakher, C. Experimental investigation on butane diffusion flames under the influence of magnetic field by using digital speckle pattern interferometry. *Appl. Opt.* **2015**, *54*, 2450–2460. [[CrossRef](#)]
- Henshaw, P.F.; D'andrea, T.; Mann, K.R.C.; Ting, D.S.-K. Premixed ammonia-methane-air combustion. *Combust. Sci. Technol.* **2005**, *177*, 2151–2170. [[CrossRef](#)]
- Aoki, T. A Magnetically Induced Anomalous Ring Flame and Quenching Characteristics of Butane Flames. *Jpn. J. Appl. Phys.* **1990**, *29*, 864–867. [[CrossRef](#)]
- Ueno, S.; Harada, K. Effects of magnetic fields on flames and gas flow. *IEEE Trans. Magn.* **1987**, *23*, 2752–2754. [[CrossRef](#)]
- Wu, W.F.; Qu, J.; Zhang, K.; Chen, W.P.; Li, B.W. Experimental studies of magnetic effect on methane laminar combustion characteristics. *Combust. Sci. Technol.* **2016**, *188*, 472–480. [[CrossRef](#)]
- Mizutani, Y.; Fuchihata, M.; Ohkura, Y. Pre-mixed laminar flames in a uniform magnetic field. *Combust. Flame* **2001**, *125*, 1071–1073. [[CrossRef](#)]
- Agarwal, S.; Kumar, M.; Shakher, C. Experimental investigation of the effect of magnetic field on temperature and temperature profile of diffusion flame using circular grating talbot interferometer. *Opt. Lasers Eng.* **2015**, *68*, 214–221. [[CrossRef](#)]

16. Gupta, A.; Baker, J. Uniform Magnetic Fields and Equilibrium Flame Temperatures. *J. Thermophys. Heat Transf.* **2007**, *21*, 520–524. [[CrossRef](#)]
17. Pandey, P.K.; Kumar, M.; Kumar, V.; Shakher, C. Measurement of temperature and temperature profile of wick stabilized micro diffusion flame under the effect of magnetic field using digital speckle pattern interferometry. *Opt. Eng.* **2017**, *56*, 14106. [[CrossRef](#)]
18. Agarwal, S.; Shakher, C. Effect of magnetic field on temperature profile and flame flow characteristics of micro flame using Talbot interferometer. *Optik* **2018**, *168*, 817–826. [[CrossRef](#)]
19. Agarwal, S.; Kumar, V.; Shakher, C. Temperature measurement of wick stabilized micro diffusion flame under the influence of magnetic field using digital holographic interferometry. *Opt. Lasers Eng.* **2018**, *102*, 161–169. [[CrossRef](#)]
20. Kumar, V.; Rastogi, V.; Agarwal, S.; Shakher, C. Investigation of temperature profile and temperature stability of micro diffusion flame under the influence of magnetic field by use of a holo-shear lens-based interferometer. *Opt. Eng.* **2020**, *59*, 064107. [[CrossRef](#)]
21. Yamada, E.; Shinoda, M.; Yamashita, H.; Kitagawa, K. Experimental and numerical analyses of magnetic effect on OH radical distribution in a hydrogen-oxygen diffusion flame. *Combust. Flame* **2003**, *135*, 365–379. [[CrossRef](#)]
22. Yamada, E.; Shinoda, M.; Yamashita, H.; Kitagawa, K. Influence of Four Kinds of Gradient Magnetic Fields on Hydrogen-Oxygen Flame. *AIAA J.* **2003**, *41*, 1535–1541. [[CrossRef](#)]
23. Shinoda, M.; Yamada, E.; Kajimoto, T.; Yamashita, H.; Kitagawa, K. Mechanism of magnetic field effect on OH density distribution in a methane-air premixed jet flame. *Proc. Combust. Inst.* **2005**, *30*, 277–284. [[CrossRef](#)]
24. Kajimoto, T.; Yamada, E.; Shinoda, M.; Kitagawa, K. Magnetic Effect on a Methane-Air Premixed Flame in Air or Nitrogen Atmosphere. In Proceedings of the 1st International Energy Conversion Engineering Conference (IECEC), Portsmouth, VA, USA, 17–21 August 2003.
25. Wakayama, N.I.; Ito, H.; Kuroda, Y.; Fujita, O.; Ito, K. Magnetic support of combustion in diffusion flames under microgravity. *Combust. Flame* **1996**, *107*, 187–188, 189–192. [[CrossRef](#)]
26. Gilard, V.; Gillon, P.; Blanchard, J.-N.; Sarh, B. Influence of a Horizontal Magnetic Field on a Co-Flow Methane/Air Diffusion Flame. *Combust. Sci. Technol.* **2008**, *180*, 1920–1935. [[CrossRef](#)]
27. Wakayama, N.I. Effect of a gradient magnetic field on the combustion reaction of methane in air. *Chem. Phys. Lett.* **1992**, *188*, 279–281. [[CrossRef](#)]
28. Ueno, S. Quenching of flames by magnetic fields (abstract). *J. Appl. Phys.* **1988**, *64*, 6030. [[CrossRef](#)]
29. Gillon, P.; Badat, W.; Gilard, V.; Sarh, B. Magnetic Effects on Flickering Methane/Air Laminar Jet Diffusion Flames. *Combust. Sci. Technol.* **2016**, *188*, 1972–1982. [[CrossRef](#)]
30. Baker, J.; Calvert, M.E. A study of the characteristics of slotted laminar jet diffusion flames in the presence of non-uniform magnetic fields. *Combust. Flame* **2003**, *133*, 345–357. [[CrossRef](#)]
31. Khaldi, F.; Messadek, K.; Benselama, A.M. Isolation of Gravity Effects on Diffusion Flames by Magnetic Field. *Microgravity Sci. Technol.* **2008**, *22*, 1–5. [[CrossRef](#)]
32. Zake, M.; Barmina, I.; Buceniaks, I.; Krishko, V. Magnetic field control of combustion dynamics of the swirling flame flow. *Magnetohydrodynamics* **2010**, *46*, 171–186.
33. Zhen, H.; Wang, Z.; Liu, X.; Wei, Z.; Huang, Z.; Leung, C. An experimental study on the effect of DC electric field on impinging flame. *Fuel* **2020**, *274*, 117846. [[CrossRef](#)]
34. Khaldi, F.; Noudem, J.; Gillon, P. On the similarity between gravity and magneto-gravity convection within a non-electroconducting fluid in a differentially heated rectangular cavity. *Int. J. Heat Mass Transf.* **2005**, *48*, 1350–1360. [[CrossRef](#)]
35. Khaldi, F. Controlling Gravity Impact on Diffusion Flames by Magnetic Field. *J. Heat Transf.* **2012**, *134*, 061201. [[CrossRef](#)]
36. Kittel, C. Introduction to Solid State Physics. *Am. J. Phys.* **1953**, *21*, 650. [[CrossRef](#)]
37. Gillon, P.; Blanchard, J.N.; Gilard, V. Methane/Air-Lifted Flames in Magnetic Gradients. *Combust. Sci. Technol.* **2010**, *182*, 1805–1819. [[CrossRef](#)]
38. Fähnle, M.; Souletie, J. The Generalized Curie-Weiss Law. *Phys. Status Solidi* **1986**, *138*, 181–188. [[CrossRef](#)]
39. Zhang, G.; Xia, T.; Xue, L.; Zhang, X. Extension of Curie-Weiss law. *Phys. Lett. A* **2006**, *360*, 327–329. [[CrossRef](#)]
40. GroÑ, T.; Pacyna, A.W.; Malicka, E. Influence of Temperature Independent Contribution of Magnetic Susceptibility on the Curie-Weiss Law. *Solid State Phenom.* **2011**, *170*, 213–218. [[CrossRef](#)]